• Basic Research •

MicroRNA-26a-5p inhibits high glucose-induced Müller cells apoptosis by mediating PTEN/PI3K/Akt pathway

Rui Shi[1], *De–Rong Tang*[2], *Di Li*[1], *Yu–Wen Yang*[3], *Hong–Bo Li*[4], *Dan–Dan Liu*[5], *Xiao–Yu Gong*[6], *Jing Qin*[1]

[1]Department of Ophthalmology, Shaanxi Provincial People's Hospital, Xi'an 710068, Shaanxi Province, China
[2]Department of Ophthalmology, Medical College of Ankang Vocational and Technical College (Ankang Central Hospital), Ankang 725000, Shaanxi Province, China
[3]The Molecular Neuropharmacology Laboratory and the Eye-Brain Research Center, The State Key Laboratory of Ophthalmology, Optometry and Visual Science, Eye Hospital, Wenzhou Medical University, Wenzhou 325027, Zhejiang Province, China
[4]School of Basic Medical Sciences, Xi'an Medical University, Xi'an 710061, Shaanxi Province, China
[5]Department of Ophthalmology, Xi'an Aier Ancient City Eye Hospital, Xi'an 710018, Shaanxi Province, China
[6]Department of Ophthalmology, The First Affiliated Hospital of Xi'an Medical University, Xi'an 710005, Shaanxi Province, China
Co-first Authors: Rui Shi and De-Rong Tang
Correspondence to: Jing Qin. Department of Ophthalmology, Shaanxi Provincial People's Hospital, Xi'an 710068, Shaanxi Province, China. qinjing20230223@163.com
Received: 2025-08-18 Accepted: 2026-07-01

Abstract

• **AIM:** To investigate the functions of microRNA-26a-5p (miR-26a-5p) in the high glucose (HG)-induced rat retinal Müller cells (rMC-1) apoptosis and its possible mechanism.

• **METHODS:** rMC-1 cells were transfected with miR-26a-5p mimics or phosphatase and tensin homolog (PTEN) siRNA under HG conditions. Cell apoptosis was analyzed by propidium iodide (PI) and annexin V fluorescein isothiocyanate (FITC) staining. PTEN/phosphatidylinositol 3-kinase (PI3K)/protein kinase B (Akt) pathway activation was assessed by quantitative reverse transcription polymerase chain reaction (qRT-PCR) and Western blot. Inflammatory cytokines, interleukin (IL)-1β, IL-6, were measured by enzyme-linked immunosorbent assay (ELISA). The miR-26a-5p-PTEN interaction was validated by dual-luciferase assay.

• **RESULTS:** HG significantly suppressed miR-26a-5p expression and induced apoptosis in rMC-1 cells. Overexpression of miR-26a-5p attenuated HG-induced apoptosis by directly targeting PTEN, as confirmed by dual-luciferase reporter assay, which demonstrated that miR-26a-5p directly binds to the PTEN 3'-UTR, resulting in a 50% reduction in luciferase activity (P<0.01). Consistent with this, miR-26a-5p overexpression downregulated PTEN expression, enhanced PI3K/Akt phosphorylation, and suppressed the secretion of IL-1β and IL-6 (all P<0.01).

• **CONCLUSION:** Upregulation of miR-26a-5p protects rMC-1 from HG-induced apoptosis by targeting PTEN *via* regulating the PI3K/Akt pathway and inflammatory responses. miR-26a-5p may be a potential therapeutic target for diabetic retinal neurodegeneration.

• **KEYWORDS:** microRNA-26a-5p; phosphatase and tensin homolog; Müller cell; PI3K/Akt pathway; apoptosis; high glucose

DOI:10.18240/ijo.2026.10.06

Citation: Shi R, Tang DR, Li D, Yang YW, Li HB, Liu DD, Gong XY, Qin J. MicroRNA-26a-5p inhibits high glucose-induced Müller cells apoptosis by mediating PTEN/PI3K/Akt pathway. *Int J Ophthalmol* 2026;19(10):1929-1938

INTRODUCTION

Diabetic retinopathy (DR) is a prevalent complication of diabetes mellitus and continues to be a major cause of visual loss worldwide. Over the years, research on DR has mostly concentrated on retinal microvascular dysfunction[1]. Nevertheless, an increasing amount of evidence indicates that retinal neurodegeneration is an initial event in the development of DR[2-3]. Additionally, within the neuroretina, the structural and functional alterations occur earlier than those in the microvascular system lesions visible in fundus images[4-5]. Müller cells are considered the primary glial cells found in the retina, which span the full thickness of the tissue and envelop all retinal neurons and blood vessels[6-7]. It has been demonstrated that Müller cell apoptosis and the secretion of inflammatory cytokines are significant factors in the development of diabetic retinal neurodegeneration, which will promote retinal microvascular disease progression[8]. However,

the fundamental process remains largely unclear. Therefore, it is essential to acquire a deeper understanding of cell apoptosis progression in retinal Müller cells caused by high glucose (HG). This knowledge might lead to the establishment of new therapeutic approaches and enhance DR treatment.

MicroRNAs (miRNAs) are a family of small non-coding RNAs that have the capacity to regulate fundamental biological processes, encompassing angiogenesis and cell apoptosis, *via* regulating their target genes and signal pathways[9]. Several miRNAs have been shown to be essential regulators of cellular apoptosis and are implicated in the progression of diabetic retinal neurodegeneration. MicroRNA-26a-5p (miR-26a-5p), belonging to the miRNAs family, regulates cell differentiation, proliferation, and apoptosis. In the context of DR, emerging evidence suggests that miR-26a-5p is dysregulated and may contribute to both neuronal and vascular pathology. It achieves this by directly controlling its target gene expression, phosphatase and tensin homolog (PTEN) in order to modulate various signaling pathways. Furthermore, it has emerged that plasma miR-26a-5p is a biomarker that may indicate the early stages of retinal neurodegeneration in DR. Additionally, our prior work has established that miR-26a-5p has a vital involvement in controlling PTEN expression in diabetic mice with retinal neurodegeneration. Nevertheless, in retinal Müller cells, the precise involvement of miR-26a-5p/PTEN in promoting cell apoptosis under HG circumstances and the following signaling pathways involved is not yet fully understood.

The phosphatidylinositol 3-kinase (PI3K)/protein kinase B (Akt) signaling pathway is a critical biological mechanism responsible for regulating the cell cycle progression. Multiple investigations have demonstrated that the PI3K/Akt pathway possesses a regulatory function in neurological disorders[10]. Activation of this pathway also provides neuroprotective benefits in individuals with Alzheimer's disease[11]. PTEN is a well-established suppressor of the PI3K/Akt pathway. Although the PTEN/PI3K/Akt axis is known to be involved in diabetic complications, its specific regulation by miR-26a-5p in Müller glia under DR conditions remains largely unexplored. To our knowledge, it has not been reported whether miR-26a-5p modulates HG-induced apoptosis in Müller cells by targeting PTEN and consequently regulating PI3K/Akt signaling. This investigation aims to elucidate the regulatory effect of miR-26a-5p and its following signal pathways in HG-induced retinal Müller cells apoptosis.

MATERIALS AND METHODS

Ethical Approval All experimental protocols were approved by the Shaanxi Provincial People's Hospital Ethics Committee (No.2021-101) and complied with relevant guidelines.

Cell Cultures and Identification The Rat Müller cell line (rMC-1) was provided by Dr. Liu-Mei Hu from Peking Union Medical College Hospital. rMC-1 was cultured in HG supplemented Dulbecco's Modified Eagle Medium (DMEM; Gibco, Grand Island, NY, USA) with 10% fetal bovine serum (FBS; Gibco, Grand Island, NY, USA) and 1% penicillin/streptomycin. The culture was preserved in a constant temperature incubator at 37°C under 5% CO_2. The 293 T cells, which are human renal epithelial cells, were obtained from the Stem Cell Bank of the Chinese Academy of Sciences (Shanghai, China). The cells were cultivated in DMEM (Gibco) containing 10% FBS and 1% penicillin/streptomycin. The culture was maintained at a temperature of 37°C in a humidified environment with 5% CO_2. At a concentration of $(5–6)\times10^4$/mL, the cells were placed in 6-well plates incubated for 24h and prepared for cell-specific markers-glutamine synthetase (GS) immunofluorescence analyses. rMC-1 apoptosis model was stimulated with 50 mmol/L of HG.

Cell Transfection and Treatment The negative control (NC), inhibitor, and miR-26a-5p compounds were acquired from BoTian company (Suzhou, China) and introduced into cells on the basis of manufacturer's recommendations employing Lipofectamine 2000 (Invitrogen, Carlsbad, CA, USA). Once the cells had grown to 80% confluence, they were placed in a 50 mmol/L glucose solution, and left to incubate for 48h. Prior to further experimental examination, the cells were halted in growth by incubating them with serum-free media overnight. Subsequently, they were incubated with either 5.5 mmol/L glucose (normal glucose, from Sigma, St. Louis, MO, USA) or 50 mmol/L glucose (HG) for 48h. The cell medium was gathered and preserved at a temperature of -80°C following the treatment.

Immunofluorescence After placing rMC-1 cells in 24-well cell slides, they were subjected to fixation by treating them with a 4% paraformaldehyde solution for 20min at ambient temperature. Immunofluorescence was conducted employing the same methods as previously explained. The antibodies included rabbit anti-GS, anti-PTEN, and goat-anti-rabbit secondary antibodies at 1:1000.

Cell Counting Kit-8 Each well of a 96-well plate was filled with 100 μL of cell solution containing 5×10^4 cells. For each group, duplicate wells were created. The culture plate was incubated for 24h in the incubator to allow for preculture, during which time the cells adhered to the wells. Various quantities of rMC-1 were introduced to the plate and incubated for 24h. Subsequently, normal and HG medium were introduced to the culture plate and 10 μL of the cell counting kit-8 (CCK-8) reagent (Elabscience Biotechnology Co., Ltd., Wuhan, China) was added to each well following a 24-hour incubation period. For 2h, the cells were incubated. Employing

an automated microplate reader (Epoch company, Dalian, China). Relative cell activity=(OD value of the experimental group/OD value of the control group)×100%.

Flow Cytometry for Apoptosis Analyses Propidium iodide (PI) and annexin V fluorescein isothiocyanate (FITC) stains were utilized in flow cytometry for recognizing apoptosis, following the instructions provided by the manufacturer. Following digestion with a 0.25% trypsin solution and subsequent centrifugation at 400× g for 5min, for subsequent analysis, rMC-1 cells from each experimental group were suspended in ice-cold PBS. The resuspension was treated with annexin V-FITC and PI stains and then incubated in darkness for 20min. Subsequently, the rMC-1 suspension was filtered using a 250-μm mesh to avoid aggregation prior to fluorescence and data analysis. The fluorescence emission was quantified utilizing the FACS LSR II® instrument at emission wavelength of 518 nm for annexin V-FITC and 620 nm for PI. Data were analyzed using FlowJo® VX software (Tree Star, Oregon, USA). The data analysis encompassed calculating the proportion of viable cells in the experimental group relative to the control group.

RNA Isolation and Quantitative Real-time Polymerase Chain Reaction rMC-1 cells were subjected to total RNA extraction employing the TRIzol reagent (#15596018; Invitrogen). The revert aid first strand cDNA synthesis kit (#K1622; Thermo Fisher Scientific) was employed for transforming 1 μg of RNA from each material into cDNA *via* reverse transcription. Following the manufacturer's recommendations, quantitative reverse transcription polymerase chain reaction (qRT-PCR) procedure was executed by applying an ABI 7500 real-time PCR instrument (Applied Biosystems, USA) and the power UP SYBR Green Master Mix (#A25742; Thermo Fisher Scientific). The relative expression levels of several genes, including PI3K, Akt, PTEN, and miR-26a-5p, were quantified using the $2^{-\Delta\Delta Ct}$ method. The gene-specific primers were sponsored and designed by Shanghai Kangcheng Biotech (Table 1).

Western Blot Analysis Cell lysis buffer containing PTEN, PI3K, and Akt inhibitors (Xi'an BoTian Biotech, Shaanxi Province, China) was employed to dissociate the rMC-1 cells for 30min on ice. To obtain the total protein, the specimens were subsequently centrifuged at 4℃ for 15min at 12 000× g. Employing the BCA Protein Assay Kit (Beijing Solarbio Science & Technology Co., Ltd, China), the protein concentration was determined. Protein was deposited onto an equivalent quantity of 10% SDS-PAGE gel, subsequently undergoing electrophoresis and finally being moved to polyvinylidene difluoride filter (PVDF) membranes. The membranes were subjected to an overnight incubation at 4℃ employing specific primary antibodies formulated in 5% (w/v) nonfat dried milk dissolved in TBST (20 mmol/L Tris base, pH 7.6, 150 mmol/L NaCl, 0.1% Tween-20). The antibodies applied were diluted 1:1000 for PTEN, PI3K, Akt, and β-actin. To obstruct the membranes in TBST, 5% nonfat milk was employed. Membranes were cleansed three times with TBST for a total of 10min following an hour of incubation at room temperature with peroxidase-conjugated secondary anti-rabbit antibodies (1:5000 dilution) in the blocking solution. A chemiluminescence tool with enhanced capabilities was employed to generate protein bands (GE Healthcare, Buckinghamshire, UK).

Table 1 Primers used for quantitative reverse transcription polymerase chain reaction

Genes	Primer (5'-3')
miR-26a-5p	F: ACACTCCAGCTGGGTTCAAGTAATCCAGGA
	R: TGGTGTCGTGGAGTCG
PTEN	F: AGACCATAACCCACCACAGC
	R: TGACAGGCACAACGACAACA
PTK3CA	F: TGACAGGCACAACGACAACA
	R: TTCCCATCACAAACAAGAAGTCC
AKT1	F: TCTCAGTGGCACAATGTCAGC
	R: AGTCCATCGTCTCCTCCTCC
ACTB	F: CCTGGCACCCAGCACAAT
	R: GCTGATCCACATCTGCTGGAA
U6	F: CTCGCTTCGGCAGCACA
	R: AACGCTTCACGAATTTGCGT

miR: MicroRNA; *PTEN*: Phosphatase and tensin homolog; *PIK3CA*: Phosphatidylinositol-4,5-bisphosphate 3-kinase catalytic subunit alpha (encoding the catalytic subunit of PI3K); *AKT1*: AKT serine/threonine kinase 1 (encoding Akt); *ACTB*: Actin beta (encoding β-actin); U6: U6 small nuclear RNA.

Dual-Luciferase Reporter Assay The targeting association between miR-26a-5p and PTEN was anticipated by employing bioinformatics tools available at http://www.targetscan.org. The pYr-MirTarget Luciferase vector plasmid was modified by inserting a synthetic PTEN 3'-untranslated region (3'-UTR) sequence, which contains the binding site for miR-26a-5p. In addition, a plasmid with the wild-type PTEN 3'-UTR (PTEN-WT) was generated. This served as the foundation for the development of the mutant-type plasmid PTEN 3'-UTR (PTEN-Mut). The procedure was executed in adherence to the guidelines included in the plasmid extraction kit. Following this, the cells were placed in the 96-well plate and Lipofectamine 2000 transfection was applied following the cells had grown to around 80% confluence. The process of introducing both PTEN-WT and PTEN-Mut genes, together with NC or miR-26a-5p mimics, into 293 T cells was carried out. The luciferase activity was assessed utilizing a luciferase detection reagent 48h subsequent to transfection. A minimum of three replicates of each trial were conducted, and the data

analysis utilized the mean value.

ELISA Analysis Cytokine levels [interleukin (IL)-1β and IL-6] were measured in cell culture supernatants using commercial enzyme-linked immunosorbent assay (ELISA) kits following the manufacturer's protocol. Briefly, supernatants were collected after centrifugation (1000× g, 10min, 4℃) to remove debris and stored at -80℃ until analysis. Standards and samples (100 μL/well, diluted in assay buffer) were added to antibody-precoated 96-well plates and incubated (2h, room temperature). After washing 3 times with phosphate buffered saline (PBS)-Tween, detection antibodies and streptavidin-horseradish peroxidase (HRP) were sequentially added, followed by TMB substrate incubation (15min, dark). Reactions were stopped with 2 mol/L H_2SO_4, and absorbance was read at 450 nm using a microplate reader. Data were analyzed using 4-parameter standard curves (GraphPad Prism 9.0), with quality controls including duplicate measurements (CV<12%) and high curve linearity (R^2>0.99).

Statistical Analysis All experiments were independently repeated at least 3 times with consistent conditions. Quantitative data were presented as mean±standard error of the mean (SEM) unless otherwise specified. A two-tailed unpaired *t*-test was deployed to compare two groups. For further analysis of additional data sets, a one-way analysis of variance followed by Tukey's multiple comparison post-test (unless otherwise specified) was employed to ascertain statistical significance between experimental groups. The data was analyzed employing GraphPad Prism 9 software (GraphPad Software Inc, USA). Outcomes were statistically significant when the *P*-value<0.05.

RESULTS

Retinal Müller Cell Determination and HG Concentration Screening The cultured rMC-1 cells are long and spindle-shaped and grow in an adherent manner. Cell-specific markers-GS were detected by immunofluorescence for Müller cell identification. As shown in Figure 1A, a polyclonal anti-GS antibody showed positive labeling in rMC-1, which confirmed the cells derived from retina. Then, to select appropriate concentrations of glucose and observation time points for experiments, we treated the rMC-1 cells with various concentrations of 25, 50, or 75 mmol/L glucose for 12, 24, or 48h, and cell viability was measured at each time point using the CCK-8 assay. We found that cell viability was significantly decreased following treatment with 50 mmol/L glucose for 48h (Figure 1B). We also detected the apoptosis of rMC-1 cells exposed to 50 mmol/L glucose for 12, 24, or 48h using flow cytometry (Figure 1C). Under 50 mmol/L glucose, rMC-1 cells started to show obviously increased apoptosis at 48h (Figure 1D). Therefore, the rMC-1 cells were treated with 50 mmol/L glucose for 48h in the following experiments in this study.

HG Treatment Causes Down-regulation of miR-26a-5p in rMC-1 miR-26a-5p expression alterations in rMC-1 cells that had been subjected to HG treatment were examined to ascertain the possible involvement of miR-26a-5p in DR. The findings manifested that rMC-1 hindered miR-26a-5p expression due to exposure to HG, as determined by qRT-PCR (Figure 2). The observations suggest that miR-26a-5p has a significant function in controlling HG-induced apoptosis of rMC-1.

miR-26a-5p Overexpression Mitigates HG-caused Apoptosis of rMC-1 To ascertain the miR-26a-5p function in HG-caused apoptosis regulation in rMC-1 cells, we examined the consequences of miR-26a-5p overexpression on HG-induced apoptosis. The findings indicated that the introduction of miR-26a-5p mimics by transfection upregulated miR-26a-5p expression (Figure 3A). CCK-8 assay demonstrated that that the miR-26a-5p overexpression successfully reversed the decline in cell viability caused by HG in rMC-1 cells (Figure 3B). Moreover, as a result of the miR-26a-5p upregulation, HG treatment of rMC-1 cells mitigated cell apoptosis (Figure 3C). Moreover, miR-26a-5p overexpression significantly reduced caspase-3 mRNA expression in HG-treated rMC-1 cells (*P*<0.01; Figure 3D). Representative flow cytometry plots further confirmed the reduction in apoptotic cells upon miR-26a-5p overexpression under HG conditions (Figure 3E).

PTEN is a miR-26a-5p Target Gene In order to clarify the fundamental process *via* which miR-26a-5p controls HG-induced rMC-1 apoptosis, bioinformatic analysis was employed to forecast the specific target gene that is influenced by miR-26a-5p. During our prior work, we have ascertained that PTEN is an intriguing miR-26a-5p target gene[12]. The interaction between PTEN and miR-26a-5p is facilitated *via* the conserved seed region located in the 3'-UTR (Figure 4A). A dual-luciferase reporter method was employed to ascertain if miR-26a-5p could attach to the PTEN 3'-UTR. The outcomes manifested that the elevated miR-26a-5p expression successfully inhibited the luciferase activity of the reporter vector that include the unchanged PTEN 3'-UTR. Nevertheless, the suppressive impact of miR-26a-5p on luciferase activity was eliminated (Figure 4B) when the anticipated binding sites were altered, emerging that miR-26a-5p forms a connection with the PTEN 3'-UTR *via* the expected binding sites. To verify the miR-26a-5p influence on PTEN expression in rMC-1, we conducted an examination of the miR-26a-5p implications on PTEN. The findings emerged that the miR-26a-5p suppression greatly enhanced the PTEN expression levels, while the upregulation of miR-26a-5p reduced PTEN expression in rMC-1 cells treated with HG conditions (Figure 4C, 4D).

Upregulation of miR-26a-5p Suppress PTEN and Activates PI3K/Akt Signaling PTEN has been proposed to

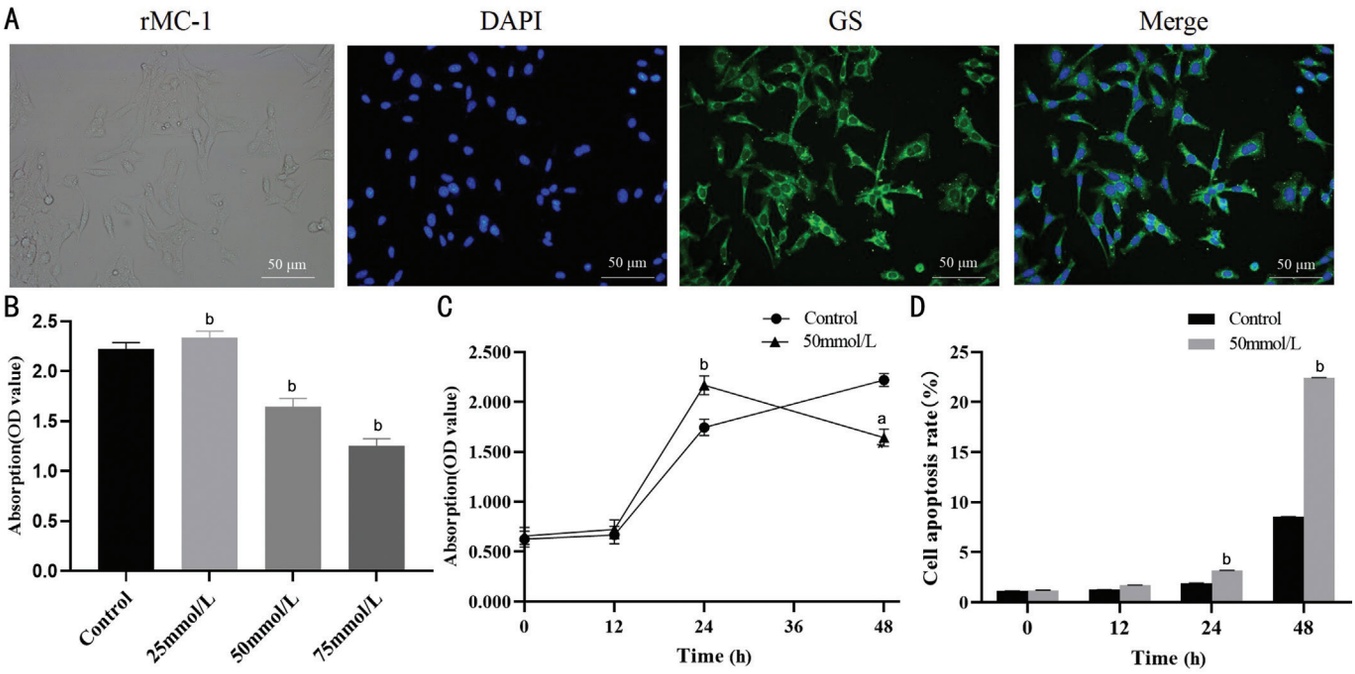

Figure 1 Retinal Müller cells identification and HG concentration screening A: Morphology and immunofluorescence identification of rMC-1 cells. Cells cultured in regular medium were stained for GS (green) and counterstained with DAPI (blue; scale bar: 50 μm, ×400 magnification). B: Glucose concentration-dependent absorption. Cells were exposed to control (5.5 mmol/L), 25, 50, or 75 mmol/L glucose to assess absorption. C: Cell viability under 50 mmol/L glucose. Viability was measured by CCK-8 assay at 12, 24, and 48h. D: The annexin V-FITC/PI double staining flow cytometry was used to detect cell apoptosis. Quantitative data: mean±SEM; *n*=5 biological replicates (3 technical replicates); [a]*P*<0.05, [b]*P*<0.01 *vs* control (one-way ANOVA with Tukey's post-hoc test). rMC-1: Rat Müller cell-1; HG: High glucose; GS: Glutamine synthetase; DAPI: 4',6-diamidino-2-phenylindole; CCK-8: Cell counting kit-8; FITC: Fluorescein isothiocyanate; PI: Propidium iodide; SEM: Standard error of the mean; ANOVA: Analysis of variance.

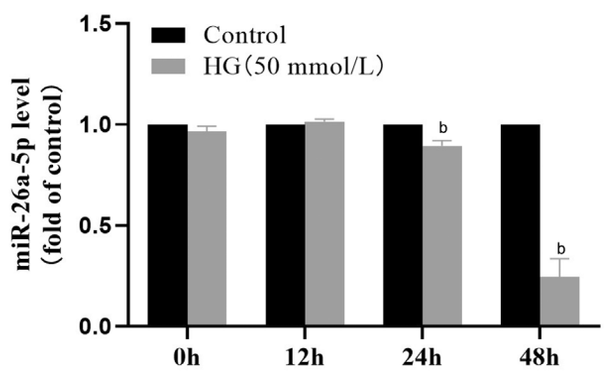

Figure 2 RT-qPCR of miR-26a-5p expression in rMC-1 cells under HG conditions Relative miR-26a-5p expression levels in rMC-1 cells treated with 50 mmol/L HG for 0, 12, 24, and 48h. Cells maintained in 5.5 mmol/L glucose served as controls. Quantitative data: mean±SEM; *n*=5 biological replicates, with each replicate containing 3 technical repeats; [b]*P*<0.01 *vs* control, two-way ANOVA with multiple comparisons test. RT-qPCR: Quantitative reverse transcription polymerase chain reaction; miR: MicroRNA; rMC-1: Rat Müller cell-1; HG: High glucose; SEM: Standard error of the mean; ANOVA: Analysis of variance.

influence cell inflammation and enhance apoptosis through its interaction with the PI3K/Akt pathway[13]. Consequently, we ascertained the implications of miR-26a-5p on the PTEN/PI3K/Akt expression. Our investigation manifested that when miR-26a-5p was elevated, it caused a significant hindrance in PTEN expression. This hindrance in PTEN expression led to the PI3K/Akt pathway activation and the production of inflammatory factors (Figure 5). The outcomes manifested that miR-26a-5p regulates the PTEN/PI3K/Akt pathway.

PTEN Knockdown Reverses the Preventive Implications of miR-26a-5p Upregulation In order to verify the PTEN involvement in the protective implications of miR-26a-5p overexpression against rMC-1 apoptosis, we examined the impact of PTEN knockdown on the protective effect caused by miR-26a-5p overexpression. We discovered that the PTEN suppression was greatly diminished *via* the miR-26a-5p overexpression, as seen by the considerable reduction in PTEN expression upon knockdown (Figure 6). The observed suppressive effects of miR-26a-5p in HG-stimulated apoptosis of rMC-1 cells were partially reversed by PTEN knockdown. Furthermore, the suppression of PTEN also eliminated the controlling implications of miR-26a-5p overexpression on the PI3K/Akt signaling pathway and the release of inflammatory factors (Figure 7). Collectively, Our findings indicate that miR-26a-5p overexpression protects rMC-1 cells against HG-induced apoptosis *via* suppressing PTEN expression.

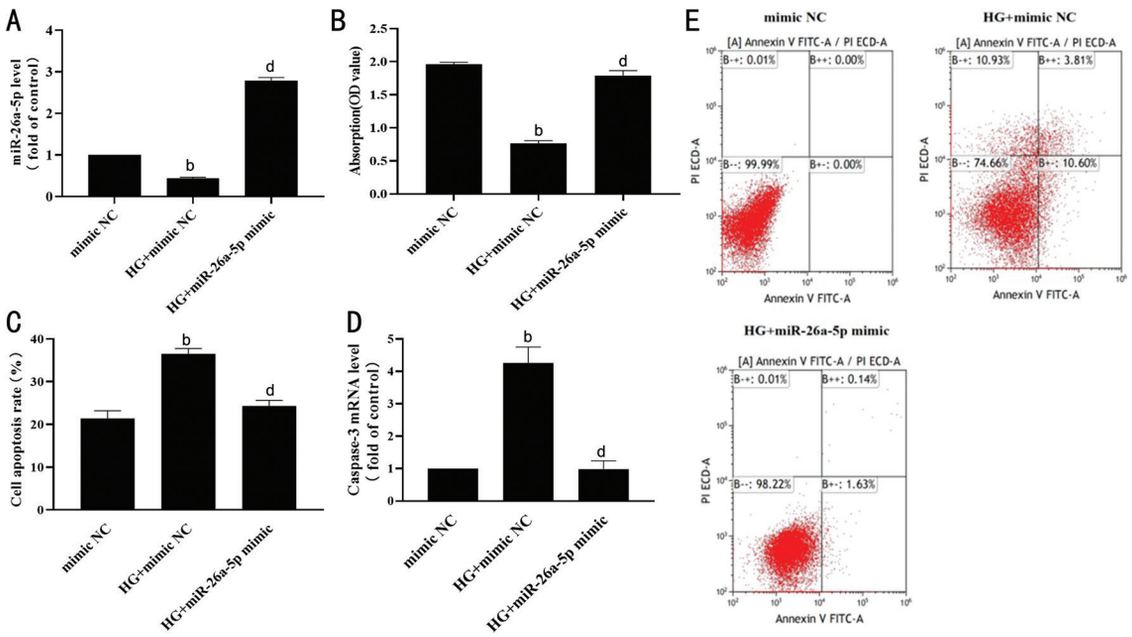

Figure 3 Overexpression of miR-26a-5p attenuates HG-induced apoptosis in rMC-1 cells rMC-1 cells were transfected with miR-26a-5p mimic for 24h and then subjected to HG-treatment for 48h. A: Relative miR-26a-5p expression levels detected by qRT-PCR after transfection with miR-26a-5p mimic. B: Cell viability assessed by CCK-8 assay following 48h HG treatment (50 mmol/L). C: Apoptosis rate measured by Annexin V-FITC/PI staining (n=3 independent experiments). D: Caspase-3 mRNA levels evaluated by qRT-PCR. Quantitative data: mean±SEM from 5 biologically independent experiments (3 technical replicates each). E: Representative flow cytometry scatter plots of Annexin V-FITC/PI staining for rMC-1 cells under different conditions. ^{b}P<0.01 *vs* mimic NC; ^{d}P<0.01 *vs* HG+mimic NC, two-way ANOVA with Tukey's post-test. miR: MicroRNA; HG: High glucose; rMC-1: Rat Müller cell-1; RT-qPCR: Quantitative reverse transcription polymerase chain reaction; CCK-8: Cell counting kit-8; FITC: Fluorescein isothiocyanate; PI: Propidium iodide; SEM: Standard error of the mean; ANOVA: Analysis of variance; NC: Negative control mimic.

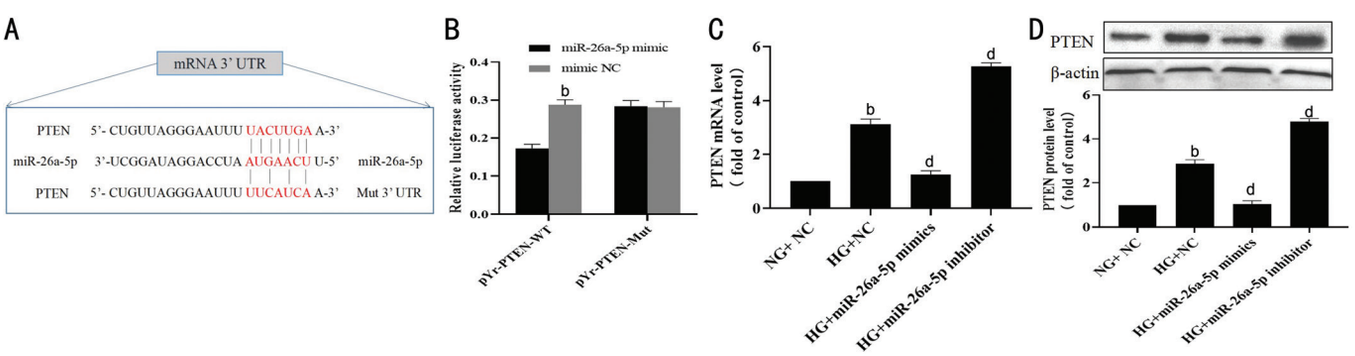

Figure 4 miR-26a-5p binds to the PTEN 3'-UTR and regulates PTEN expression A: Schematic of predicted miR-26a-5p binding sites in the PTEN 3'-UTR seed region. Mutated residues in the binding site are indicated (red). B: Dual-luciferase reporter assay in 293T cells. Cells were co-transfected with wild-type (WT) or mutant (Mut) PTEN 3'-UTR reporter vectors and miR-26a-5p mimics for 48h before detection (mean±SEM; n=5 biological replicates, each with 3 technical replicates; ^{b}P<0.01 *vs* mimic NC, two-tailed Student's t-test). C: PTEN mRNA levels in rMC-1 cells transfected with miR-26a-5p inhibitor or mimics followed by HG treatment (50 mmol/L, 48h). n=5 biological replicates, 3 technical replicates; ^{b}P<0.01 *vs* NG+NC; ^{d}P<0.01 *vs* HG+NC, one-way ANOVA with Tukey's test. D: Western blot analysis of PTEN protein expression under corresponding conditions (n=3 independent experiments; quantification normalized to β-actin; ^{b}P<0.01 *vs* NG+NC; ^{d}P<0.01 *vs* HG+NC, one-way ANOVA with Tukey's test). PTEN: Phosphatase and tensin homolog; miR: MicroRNA; UTR: Untranslated region; HG: High glucose; rMC-1: Rat Müller cell-1; SEM: Standard error of the mean; NG: Normoglycemia; NC: Negative control mimic; ANOVA: Analysis of variance.

DISCUSSION

This work demonstrates that HG downregulates miR-26a-5p in rMC-1 cells, and its overexpression protects against HG-induced apoptosis *via* the PTEN/PI3K/Akt pathway, associated with reduced inflammatory cytokine release. These findings establish miR-26a-5p as a critical regulator in diabetic retinal neurodegeneration.

The rMC-1 used in this study is a widely adopted *in vitro* model in ophthalmic research. It shares important similarities with primary Müller cells, including typical morphological characteristics, expression of specific markers (*e.g.*, glial fibrillary acidic protein and GS), and key responsive

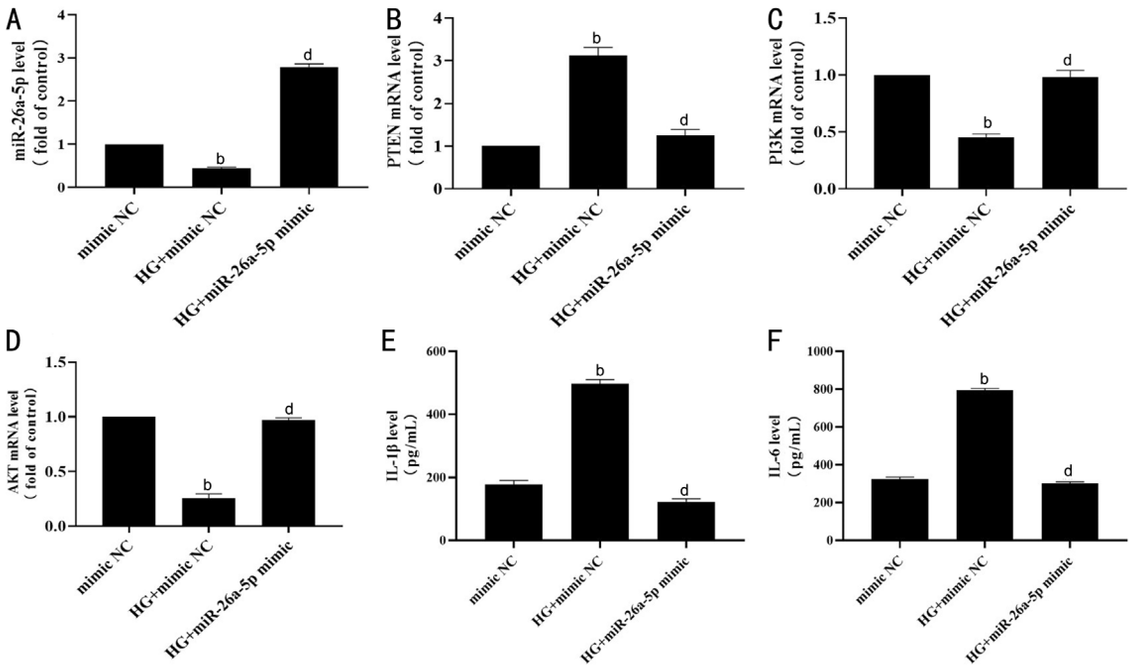

Figure 5 miR-26a-5p regulates PTEN/PI3K/Akt signaling and inflammatory factors miR-26a-5p modulates PTEN/PI3K/Akt signaling and inflammatory responses in rMC-1 cells under hyperglycemic conditions. rMC-1 were transfected with miR-26a-5p mimics for 24h and then subjected to HG treatment for 48h. A: miR-26a-5p expression levels following mimic transfection (*n*=5 biological replicates, 3 technical replicates). B–D: Relative mRNA expression of PTEN (B), PI3K (C), and Akt (D) detected by qRT-PCR (*n*=5 independent experiments, each with triplicate measurements). E–F: Secreted levels of IL-1β (E) and IL-6 (F) quantified by ELISA (*n*=3 biological replicates, duplicate measurements per sample). Mean±SEM; ^{b}P<0.01 *vs* mimic NC; ^{d}P<0.01 *vs* HG+mimic NC. One-way ANOVA with Tukey's post-hoc test for B–F; two-tailed *t*-test for A. PTEN: Phosphatase and tensin homolog; miR: MicroRNA; HG: High glucose; rMC-1: Rat Müller cell-1; PI3K: Phosphatidylinositol 3-kinase; Akt: Protein kinase B; RT-qPCR: Quantitative reverse transcription polymerase chain reaction; IL: Interleukin; ELISA: Enzyme-linked immunosorbent assay; SEM: Standard error of the mean; NC: Negative control mimic; ANOVA: Analysis of variance.

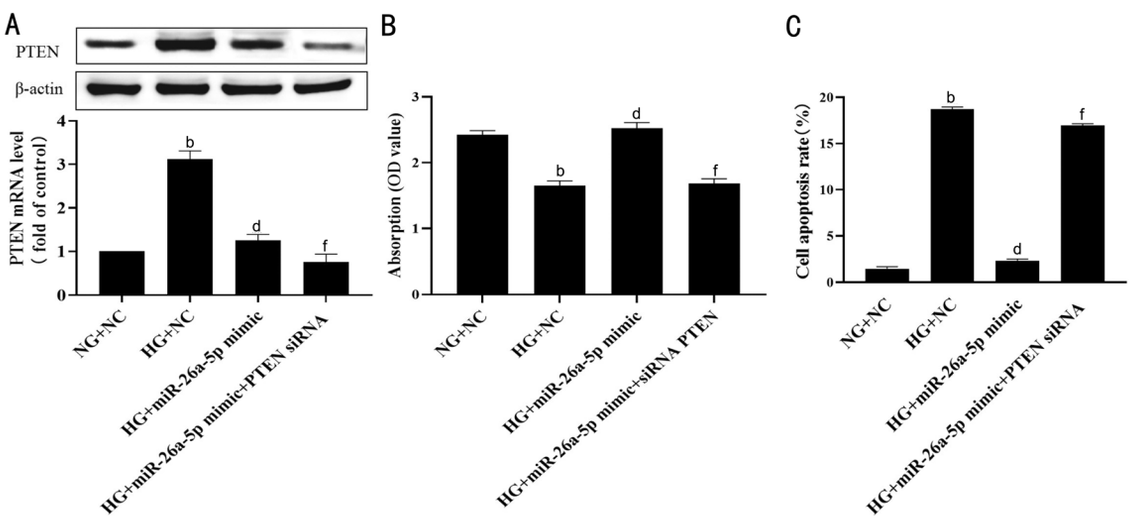

Figure 6 Knockdown of PTEN reverses the protective effect of miR-26a-5p overexpression in rMC-1 cells under hyperglycemia rMC-1 were co-transfected with miR-26a-5p mimic and PTEN siRNA for 24h and then subjected to HG treatment for 48h. A: Western blot analysis of PTEN protein expression (*n*=5 independent experiments; quantification normalized to β-actin). B: Cell viability measured by CCK-8 assay (*n*=5 biological replicates, 3 technical replicates per condition). C: Cell apoptosis rate determined by Annexin V-FITC/PI flow cytometry (*n*=3 biological replicates, ≥10 000 events analyzed per replicate). Mean±SEM; ^{b}P<0.01 *vs* NG+NC; ^{d}P<0.01 *vs* HG+NC; ^{f}P<0.01 *vs* HG+miR-26a-5p mimic. One-way ANOVA with Tukey's post-hoc test. PTEN: Phosphatase and tensin homolog; miR: MicroRNA; HG: High glucose; rMC-1: Rat Müller cell-1; CCK-8: Cell counting kit-8; FITC: Fluorescein isothiocyanate; PI: Propidium iodide; SEM: Standard error of the mean; NG: Normoglycemia; NC: Negative control mimic; ANOVA: Analysis of variance.

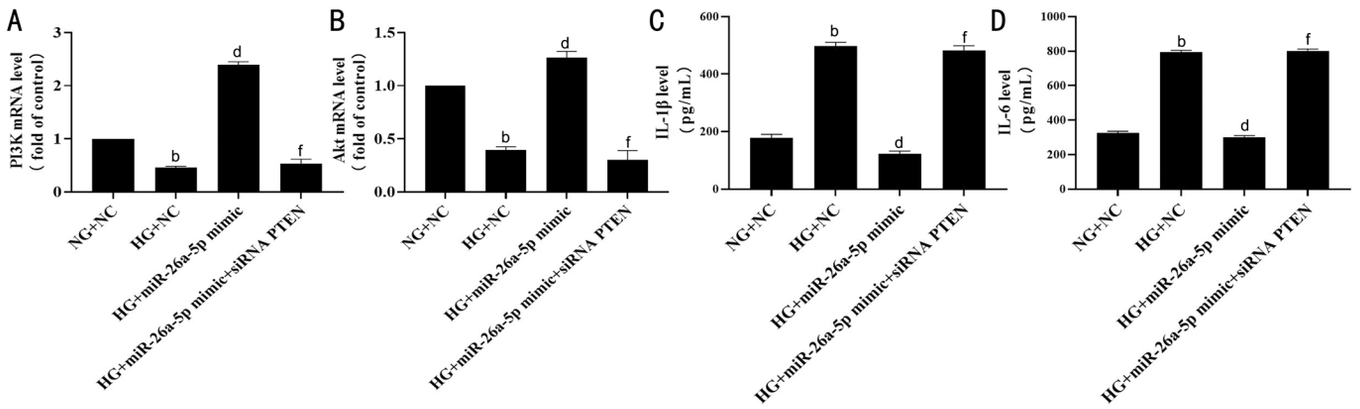

Figure 7 PTEN knockdown abrogates miR-26a-5p-mediated regulation of PI3K/Akt signaling and inflammation in rMC-1 cells A–B: Relative mRNA expression of PI3K (A) and Akt (B) detected by qRT-PCR (n=5 biological replicates, each with 3 technical replicates). C–D: Secreted levels of IL-1β (C) and IL-6 (D) quantified by ELISA (n=3 independent experiments, duplicate measurements per condition). Mean±SEM; ^{b}P<0.01 *vs* NG+NC; ^{d}P<0.01 *vs* HG+NC; ^{f}P<0.01 *vs* HG+miR-26a-5p mimic group (one-way ANOVA with Tukey's post-hoc test). PTEN: Phosphatase and tensin homolog; miR: MicroRNA; HG: High glucose; rMC-1: Rat Müller cell-1; PI3K: Phosphatidylinositol 3-kinase; Akt: Protein kinase B; RT-qPCR: Quantitative reverse transcription polymerase chain reaction; IL: Interleukin; ELISA: Enzyme-linked immunosorbent assay; SEM: Standard error of the mean; NG: Normoglycemia; NC: Negative control mimic; ANOVA: Analysis of variance.

mechanisms to HG stimulation, making it a reliable tool for investigating the molecular mechanisms of DR. Although immortalized cell lines cannot fully replicate the complexity of the *in vivo* microenvironment, the experimental conditions in this study were strictly controlled and independently repeated to ensure reproducibility and scientific rigor. Regarding the HG model, treatment with 50 mmol/L glucose is well established as an effective method for mimicking diabetic metabolic conditions. It can induce critical pathological processes-such as oxidative stress, inflammatory responses, and cellular dysfunction, that are consistent with *in vivo* disease phenotypes. The observed regulatory effects of the miR-26a-5p/PTEN/PI3K/Akt signaling axis and the apoptosis-inflammatory phenotypes in this model not only align with clinical features of DR but also provide a solid *in vitro* foundation for further mechanistic exploration and drug screening. Future studies will integrate primary cell and animal experiments to deepen the understanding of this pathway in a physiological context.

miR-26a-5p has been established as a key regulator of apoptosis across multiple pathological contexts, particularly in ophthalmic diseases[14-15]. Previous studies have demonstrated its neuroprotective role in chronic dopaminergic neuron degeneration[16-17] and its dysregulation in diabetic patients[18], suggesting potential as a diagnostic biomarker for early DR[19]. Importantly, our group has contributed to this field by showing that miR-26a-5p protects against retinal neuronal damage in diabetic mice[20] and prevents myocardial injury in diabetic rats through PTEN regulation[21-22]. While these *in vivo* studies established the therapeutic potential of miR-26a-5p in diabetes complications, the specific mechanisms in retinal Müller cells, the major glial cells responsible for DR pathogenesis, remained unexplored. The present study bridges this critical knowledge gap through three key findings: First, we identified that HG treatment significantly downregulates miR-26a-5p in rMC-1 cells, mirroring its decreased expression observed in diabetic retinas. Second, we demonstrated that miR-26a-5p overexpression effectively inhibits HG-induced apoptosis in rMC-1 cells, confirming its cytoprotective function in this specific cell type. Third, mechanistic studies revealed that this protection is mediated through PTEN/PI3K/Akt pathway modulation, leading to reduced inflammatory cytokine release, thereby unifying our observations with previous *in vivo* findings.

Past studies found miR-26a-5p as a possible cell apoptosis suppressor by regulating its target genes[23]. In our previous investigation, we predicted that PTEN is an achievable gene that may be targeted with miR-26a-5p[12] and up-regulation reversed retinal thinning via down-regulating PTEN in diabetic mice. Recently, PTEN has made a significant contribution to both diabetes mellitus and its associated comorbidities. Subsequent investigations demonstrated that miR-26a-5p hinders cell proliferation and facilitates cell apoptosis by suppressing PTEN expression[24-25]. Nevertheless, the specific connection between miR-26a-5p and PTEN in diabetic retinal neurodegeneration, as well as the possible involvements of miR-26a-5p/PTEN in HG-induced apoptosis of Müller cells, have not been thoroughly elucidated. In this investigation, it was shown that the miR-26a-5p levels fell and PTEN rose in Müller cells treated with HG, which is in line with prior research findings. Our analysis revealed that, miR-26a-5p directly targets PTEN, as evidenced by 3'-UTR luciferase

assays and PTEN expression suppression. This interaction is functionally critical, since PTEN knockdown abolished miR-26a-5p's anti-apoptotic effects.

Since PTEN is a known negative regulator of the PI3K/Akt pathway[26], we next investigated whether miR-26a-5p's protection involves PI3K/Akt activation. Indeed, miR-26a-5p-mediated PTEN suppression significantly enhanced PI3K/Akt phosphorylation[27]. Moreover, PTEN/PI3K/Akt signaling regulates various cells survival *via* influencing cell inflammation, including retinal neurons[28]. In this investigation, we manifested that downregulation of PTEN by miR-26a-5p upregulation promoted activation of PI3K/Akt and decreased pro-inflammatory cytokine release. However, PTEN knockdown abolished the suppressive implications of miR-26a-5p overexpression on Müller cell apoptosis and pro-inflammatory cytokine production. Our data suggests that apoptosis of rMC-1 triggered by HG is mediated *via* the interaction between miR-26a-5p/PTEN and PI3K/Akt pathways. Therefore, targeting miR-26a-5p might be a promising approach to regulate PTEN expression in the therapy of diabetic retinal neurodegeneration.

Our *in vitro* findings demonstrated that miR-26a-5p overexpression attenuates HG-induced apoptosis in rMC-1 through PTEN downregulation, subsequently modulating the PI3K/Akt pathway and inflammatory cytokine release. These results provide mechanistic insights into potential neuroprotective pathways in diabetic retinal cells and suggest that miR-26a-5p merits further investigation as a candidate therapeutic target for DR. However, future studies using animal models and clinical samples will be essential to validate these observations and evaluate translational potential.

This study has certain limitations that should be acknowledged; however, its scientific rationale and empirical foundation remain robust. Although the rMC-1 cell model recapitulates core functional features of Müller cells and demonstrates good reproducibility, it does not fully represent the complexity of the *in vivo* microenvironment. Further validation using primary cells or animal models is therefore warranted. The HG (50 mmol/L) treatment effectively mimics diabetic metabolic stress, yet it cannot fully capture hemodynamic and systemic regulatory factors involved in DR. Furthermore, while this study focused on the role of the miR-26a-5p/PTEN/PI3K/Akt pathway in apoptosis and inflammation, crosstalk with other signaling pathways was not systematically investigated. Lastly, due to resource constraints, phosphorylation levels of PI3K/Akt were not examined, although consistent functional and molecular evidence strongly supports our conclusions. Despite these limitations, this work provides systematic and foundational insights into the role of miR-26a-5p in DR through a mechanistically clear experimental design and convergence of multiple lines of evidence. Moving forward, we will prioritize *in vivo* validation, phosphoproteomic profiling, and investigation of cross pathway interactions to further extend and deepen these findings.

ACKNOWLEDGEMENTS

Authors' Contributions: Shi R and Tang DR contributed equally to this work and should be considered co-first authors. Shi R drafted the manuscript and performed the experiments. Tang DR contributed to data collection and analysis. Li D and Yang YW participated in the experimental design and data interpretation. Li HB and Liu DD provided technical support and contributed to statistical analysis. Gong XY and Qin J supervised the study and revised the manuscript critically for important intellectual content. All authors read and approved the final manuscript.

Data Availability Statement: The primary datasets and analysis may be obtained from the corresponding author upon a reasonable request.

AI-Generated Content Disclosure: No artificial intelligence (AI) tools or AI-assisted technologies were used in any stage of this study, including data collection, analysis, interpretation, or manuscript preparation. The authors take full responsibility for all content of this work.

Foundations: Supported by the Natural Science Foundation of Shaanxi Province in China (No.2022JM-571; No.2023-YBSF-601); Shaanxi Provincial People's Hospital (No.2021YJY-20).

Conflicts of Interest: Shi R, None; **Tang DR,** None; **Li D,** None; **Yang YW,** None; **Li HB,** None; **Liu DD,** None; **Gong XY,** None; **Qin J,** None.

REFERENCES

1 Action to Control Cardiovascular Risk in Diabetes Follow-On ACCORDION Eye Study Group and the Action to Control Cardiovascular Risk in Diabetes Follow-On ACCORDION Study Group. Persistent effects of intensive glycemic control on retinopathy in type 2 diabetes in the action to control cardiovascular risk in diabetes (ACCORD) follow-on study. *Diabetes Care* 2016;39(7):1089-1100.

2 Sung JY, Kim JJ, Hwang JY, *et al*. Retinal neurodegeneration in diabetic retinopathy with systemic hypertension. *Acta Diabetol* 2024;61(4):495-504.

3 Reste-Ferreira D, Marques IP, Santos T, *et al*. Retinal neurodegeneration in eyes with NPDR risk phenotypes: a two-year longitudinal study. *Acta Ophthalmol* 2024;102(4):e539-e547.

4 Antonetti DA, Silva PS, Stitt AW. Current understanding of the molecular and cellular pathology of diabetic retinopathy. *Nat Rev Endocrinol* 2021;17(4):195-206.

5 Zhang Y, Huang W, Tian Q, *et al*. Network pharmacology and biochemical experiments reveal the antiapoptotic mechanism of huperzine A for treating diabetic retinopathy. *Br J Ophthalmol* 2024;108(7):989-998.

6 Ghaseminejad F, Kaplan L, Pfaller AM, *et al*. The role of Müller cell glucocorticoid signaling in diabetic retinopathy. *Graefes Arch Clin Exp Ophthalmol* 2020;258(2):221-230.

7 Arrigo A, Cremona O, Aragona E, *et al*. Müller cells trophism and pathology as the next therapeutic targets for retinal diseases. *Prog Retin Eye Res* 2025;106:101357.

8 Tu Y, Zhu M, Wang Z, *et al*. Melatonin inhibits Müller cell activation and pro-inflammatory cytokine production *via* upregulating the MEG3/miR-204/Sirt1 axis in experimental diabetic retinopathy. *J Cell Physiol* 2020;235(11):8724-8735.

9 Hosseinpoor Z, Soheili ZS, Davari M, *et al*. Crosstalk between MIR-96 and IRS/PI3K/AKT/VEGF cascade in hRPE cells; A potential target for preventing diabetic retinopathy. *PLoS One* 2024;19(9): e0310999.

10 Xi X, Wang X, Ma J, *et al*. miR-130a-3p enhances autophagy through the YY1/PI3K/AKT/mTOR signaling pathway to regulate macrophage polarization and alleviate diabetic retinopathy. *J Diabetes Invest* 2025;16(3):392-404.

11 Li L, Xu Y, Zhao M, *et al*. Neuro-protective roles of long non-coding RNA MALAT1 in Alzheimer's disease with the involvement of the microRNA-30b/CNR1 network and the following PI3K/AKT activation. *Exp Mol Pathol* 2020;117:104545.

12 Shi R, Chen L, Wang W, *et al*. Plasma miR-26a-5p is a biomarker for retinal neurodegeneration of early diabetic retinopathy. *Eye* (*Lond*) 2021;35(6):1587-1599.

13 Jiang L, Cao S. Role of microRNA-26a in cartilage injury and chondrocyte proliferation and apoptosis in rheumatoid arthritis rats by regulating expression of CTGF. *J Cell Physiol* 2020;235(2):979-992.

14 Li C, Han T, Li R, *et al*. miR-26a-5p mediates TLR signaling pathway by targeting CTGF in LPS-induced alveolar macrophage. *Biosci Rep* 2020;40(6):BSR20192598.

15 Yu XH, Liu SY, Li CF. TGF-β2-induced NEAT1 regulates lens epithelial cell proliferation, migration and EMT by the miR-26a-5p/FANCE axis. *Int J Ophthalmol* 2021;14(11):1674-1682.

16 Lu Y, Liu M, Guo X, *et al*. miR-26a-5p alleviates CFA-induced chronic inflammatory hyperalgesia through Wnt5a/CaMKII/NFAT signaling in mice. *CNS Neurosci Ther* 2023;29(5):1254-1271.

17 Li F, Wei H, Li H, *et al*. miR-26a prevents neural stem cells from apoptosis *via* β-catenin signaling pathway in cardiac arrest-induced brain damage. *Biosci Rep* 2019;39(5):BSR20181635.

18 Lafourcade CA, Fernández A, Ramírez JP, *et al*. A role for mir-26a in stress: a potential sEV biomarker and modulator of excitatory neurotransmission. *Cells* 2020;9(6):1364.

19 Wu J, Shi K, Zhang F, *et al*. A 3-miRNA risk scoring signature in early diabetic retinopathy. *J Clin Med* 2023;12(5):1777.

20 Shi R, Liu DD, Cao Y, *et al*. microRNA-26a-5p prevents retinal neuronal cell death in diabetic mice by targeting PTEN. *Curr Eye Res* 2022;47(3):409-417.

21 Chiang MH, Liang CJ, Lin LC, *et al*. miR-26a attenuates cardiac apoptosis and fibrosis by targeting ataxia–telangiectasia mutated in myocardial infarction. *J Cell Physiol* 2020;235(9):6085-6102.

22 Li R, Chen L, Yao GM, *et al*. Effects of quercetin on diabetic retinopathy and its association with NLRP3 inflammasome and autophagy. *Int J Ophthalmol* 2021;14(1):42-49.

23 Song Y, Jin D, Jiang X, *et al*. Overexpression of microRNA-26a protects against deficient β-cell function *via* targeting phosphatase with tensin homology in mouse models of type 2 diabetes. *Biochem Biophys Res Commun* 2018;495(1):1312-1316.

24 Huang Z, Xing S, Liu M, *et al*. miR-26a-5p enhances cells proliferation, invasion, and apoptosis resistance of fibroblast-like synoviocytes in rheumatoid arthritis by regulating PTEN/PI3K/AKT pathway. *Biosci Rep* 2019;39(7):BSR20182192.

25 Xing X, Guo S, Zhang G, *et al*. miR-26a-5p protects against myocardial ischemia/reperfusion injury by regulating the PTEN/PI3K/AKT signaling pathway. *Braz J Med Biol Res* 2020;53(2):e9106.

26 Liu K, Shi M, Li X, *et al*. Curcumin modulates the PTEN/PI3K/AKT pathway to alleviate inflammation and oxidative stress in PM2.5-Induced chronic obstructive pulmonary disease. *Food Chem Toxicol* 2025;201:115460.

27 Lei Y, Yang M, Li H, *et al*. miR-130b regulates PTEN to activate the PI3K/Akt signaling pathway and attenuate oxidative stress-induced injury in diabetic encephalopathy. *Int J Mol Med* 2021;48(1):141.

28 Fu C, Peng J, Ling Y, *et al*. Apigenin inhibits angiogenesis in retinal microvascular endothelial cells through regulating of the miR-140-5p/HDAC3-mediated PTEN/PI3K/AKT pathway. *BMC Ophthalmol* 2023;23(1):302.